nature cell biology

ARTICLES

# A physical and functional map of the human TNF-α/NF-κB signal transduction pathway

Tewis Bouwmeester[1,2], Angela Bauch[1], Heinz Ruffner[1], Pierre-Olivier Angrand[1], Giovanna Bergamini[1], Karen Croughton[1], Cristina Cruciat[1], Dirk Eberhard[1], Julien Gagneur[1], Sonja Ghidelli[1], Carsten Hopf[1], Bettina Huhse[1], Raffaella Mangano[1], Anne-Marie Michon[1], Markus Schirle[1], Judith Schlegl[1], Markus Schwab[1], Martin A. Stein[1], Andreas Bauer[1], Georg Casari[1], Gerard Drewes[1], Anne-Claude Gavin[1], David B. Jackson[1], Gerard Joberty[1], Gitte Neubauer[1], Jens Rick[1], Bernhard Kuster[1] and Giulio Superti-Furga[1,2]

**Signal transduction pathways are modular composites of functionally interdependent sets of proteins that act in a coordinated fashion to transform environmental information into a phenotypic response. The pro-inflammatory cytokine tumour necrosis factor (TNF)-α triggers a signalling cascade, converging on the activation of the transcription factor NF-κB, which forms the basis for numerous physiological and pathological processes. Here we report the mapping of a protein interaction network around 32 known and candidate TNF-α/NF-κB pathway components by using an integrated approach comprising tandem affinity purification, liquid-chromatography tandem mass spectrometry, network analysis and directed functional perturbation studies using RNA interference. We identified 221 molecular associations and 80 previously unknown interactors, including 10 new functional modulators of the pathway. This systems approach provides significant insight into the logic of the TNF-α/NF-κB pathway and is generally applicable to other pathways relevant to human disease.**

Postgenomic biomedical research demands the use of integrated, parallel, multi-technological approaches to obtain a holistic view and understanding of complex biological phenomena. In particular, medically relevant biological pathways that entail the concerted interactions of tens or hundreds of cellular components are predestined to become the object of such studies. Recently, a large-scale functional proteomics approach has been deployed to map cellular complexes in the yeast *S. cerevisiae*[1], but so far no human signal transduction pathway has been mapped with this approach. A comprehensive functional map of a disease pathway should permit the identification and prioritization of therapeutic targets.

Among other stimuli, the proinflammatory cytokine TNF-α triggers signalling pathways that converge on the activation of the transcription factor NF-κB (ref. 2). The mammalian NF-κB family is composed of five distinct but structurally related subunits, NF-κB1/p50, NF-κB2/p52, RelA, RelB and c-Rel, which can form various homodimeric and heterodimeric combinations, each of which might have a specific signalling function[3]. Nuclear translocation of NF-κB is controlled by signal-induced degradation of the inhibitors of NF-κB (IκBs). TNF-α activates NF-κB by means of a kinase relay module, involving the receptor-proximal kinase RIPK1, the intermediate mitogen-activated protein kinase kinase kinase (MAP3K), MAP kinase/ERK kinase kinase 3 (MEKK3) and the IκB kinase (IKK)α,β,γ signalosome[2]. Two distinct NF-κB-activating IKK modules have been described; one involving the canonical IKKα,β,γ complex and one involving an alternative complex dependent on IKKα and the MAP3K NIK[4,5]. However, several aspects of the pathway logic have remained elusive, notably that concerning signalling specificity, signal relay mechanisms and kinetics of activation. Here we describe the identification of newly observed modulators of the TNF-α/NF-κB pathway through an integrated approach of proteomic pathway mapping based on established components and their paralogues, and on functional analysis with RNA interference (RNAi).

## RESULTS

### Proteomic analysis of the TNF-α/NF-κB pathway

To identify new TNF-α/NF-κB pathway components we used the tandem affinity purification (TAP) strategy to isolate cellular complexes around 32 known and candidate components (Fig. 1a). The TAP procedure is a sensitive and selective method to purify, under close-to-physiological conditions, multiprotein complexes formed *in vivo*[1,6,7]. We TAP-tagged the TNF receptors (TNF-R1 and TNF-R2), receptor-proximal components such as TRADD, TRAF1, TRAF2, TRAF6, i-TRAF, RIPK1, RIPK2, RIPK3, several MAP3K signal relay kinases (MEKK1, MEKK3, NIK, Cot-Tpl2, TAK1 and its activator subunits TAB1 and TAB2), the IKKα, β and γ subunits including the paralogues TBK1 and IKKε, all NF-κB transcription factor subunits, NF-κB1 (p105/p50), NF-κB2 (p100/p52), RelA, RelB and c-Rel, and the IκB inhibitor subunits IκBα, β and ε to screen *in vivo* for constitutive and

[1]Cellzome AG, Meyerhofstrasse 1, 69117 Heidelberg, Germany. [2]Correspondence should be addressed to T.B. or G.S.F. (e-mail: tewis.bouwmeester@cellzome.com or giulio.superti-furga@cellzome.com).

Published online: 25 January 2004; DOI: 10.1038/ncb1086

**Table 1 Protein selected for RNAi perturbation**

| Novel interactors | Description | RNAi phenotype |
|---|---|---|
| TRAF7 | E3 Ub ligase | + |
| MARK2 | Kinase | |
| TAB2 paralogue | Adaptor | + |
| FKBP51 | Isomerase | ++ |
| TBKBP1 | Adaptor | + |
| TBKBP2 | Adaptor | |
| DIS | Adaptor | |
| ABIN | Unknown | |
| JLP | Adaptor | ++ |
| COPB2 | Trafficking component | |
| ABIN-2 | Unknown | |
| KIAA0310 | Unknown | |
| CDC4 | WD40-SCF E3 | + |
| USP9 | Ubiquitin protease | |
| GTFII-I | Transcription factor | |
| nAKAP95 | Scaffold | |
| USP11 | Ubiquitin protease | |
| HDAC6 | Deacetylase | |
| REQ | Transcription Factor | |
| BCL7A | Unknown | |
| MCC1 | Unknown | + |
| IQGAP2 | GAP | + |
| NGAP | GAP | + |
| KIAA0379 | Unknown | |
| KIAA0685 | Unknown | |
| FLJ20288 | Unknown | |
| KIAA1115 | Unknown | |
| PPP6c | Phosphatase | + |

Phenotype classification: +, 1 siRNA showing the same phenotype in at least 3 of 4 experiments; ++, ≥ 2 siRNAs showing the same phenotype in at least 3 of 4 experiments

signal-induced protein interactions. After stable integration into TNF-α-responsive HEK293 cells by retrovirus-mediated gene transfer, the tagged proteins were purified in complex with their endogenous associated proteins from uninduced and TNF-α-induced cells. Expression levels of the TAP-tagged proteins were gauged to close-to-endogenous levels by adjusting the multiplicity of infection. Any potential problem arising from mild overexpression of tagged proteins is likely to be compensated for by independent, multiple repeat experiments and reciprocal protein complex purification with other TAP-tagged complex components. This method allows the detection of endogenous, post-translationally modified proteins within their physiological context, and we did indeed observe that complex composition and post-translational modification of constituents varied in response to stimuli (Fig. 1b, c). Protein constituents were unambiguously identified by liquid-chromatography tandem mass spectrometry (LC–MS/MS). In total, the raw data set contains 680 non-redundant protein hits (Supplementary Table S1). Of the 241 interactions previously reported in the literature for the 32 pathway components chosen, 171 were identified, resulting in a benchmarking success rate of about 70%. Molecular associations that were not recapitulated here might be: (1) too transient or of too low affinity, (2) dependent on stimuli other than TNF-α, (3) prevented by steric interference of the tag, (4) due to low protein expression levels and tissue specificity or (5) experimentally unreproducible. The false-positive rate of the TAP/MS approach in mammalian cells is difficult to assess before experimental validation, but on the basis of our genome-wide saturation screen in *S. cerevisiae* we estimate it to be below 20% (refs 8, 9, and unpublished data). The fidelity of the experimental set-up is further demonstrated by the TNF-α-induced degradation of IκBα,ε and the inducible association of the Skp1/Cullin 1/F-box (SCF) E3 ubiquitin ligase complex with IκB isoforms as both measured by MS (Fig. 1b). In total, 33 interactors were dependent on a stimulus (TNF-α or NIK) (Fig. 2, Supplementary Table S4).

In addition to the identification of components of protein complexes by mass spectrometry, intriguing observations around post-translational modifications were made. Notably, conjugation with Nedd8 ('neddylation') was consistently and exclusively observed for Cullin-1 and Cullin-2, the catalytic subunits of the SCF E3 ubiquitin ligase, after stimulation with TNF-α (data not shown). In addition, we also observed numerous TNF-α-induced ubiquitination events. As expected, these included the IκBs, the NF-κB precursors p105 and p100, but also others such as c-Rel, RelA and TAK1.

## A physical map

In total, 237 TAP purifications (at least four purifications per TAP-tagged component) and subsequent LC–MS/MS analysis led to a large network of 680 non-redundant proteins that were identified at least twice. To deconvolve the complexity of the dataset, we applied a stringent statistical analysis based on specificity and consistency, by comparison against a control dataset of 233 non-TNF-α pathway-related TAP experiments from HEK293 cells. The resulting filtered network is composed of 131 high-confidence interactors, 80 of which are new and might have specific roles in stimulus-dependent NF-κB signalling cascades (Supplementary Table S2). This network formed the basis for further analysis. A physical connectivity graph was constructed to position and correlate these new interactors with the known TNF-α/NF-κB pathway components (Fig. 2). In this graph, proteins are symbolized according to the Alliance for Cellular Signalling convention, with TAP-tagged components framed in green. The remainder of the interactors, available online (http://tnf.cellzome.com), include: (1) proteins at the interface of the cellular life-cycle of pathway components that also occur in other signalling pathways, (2) possible experimental artefacts caused by disruption of the cellular compartmentalization during lysis and (3) highly abundant contaminants. Apart from recapitulating most of all previously suggested physical relationships, we observed intriguing clustering of specific new interactors around pathway components that provide mechanistic insight into NF-κB signalling properties, such as transcription factor specificity, inhibitor specificity and precursor processing. Interactors that are stimulus-dependent (TNF-α and NIK) are highlighted in the graph.

With regard to transcription factor specificity we found that RelB interacted constitutively with the SWI/SNF chromatin remodelling complex, composed of nine subunits, histone deacetylase 6, the lymphoid transcription factor REQ and the ubiquitin protease USP11. The specific chromatin components might explain the unique functions of RelB among the NF-κB family members in the activation of late response genes[10]. Besides a pronounced and expected preference for RelA and c-Rel-containing complexes, both IκBβ and IκBε co-purified with proteins that might control the kinetics of their proteolytic degradation (MCC1 and NGAP for IκBβ, and PPP6c, KIAA0379 and FLJ20288 for IκBε), akin to the role of κB–Ras in stabilizing IκBβ

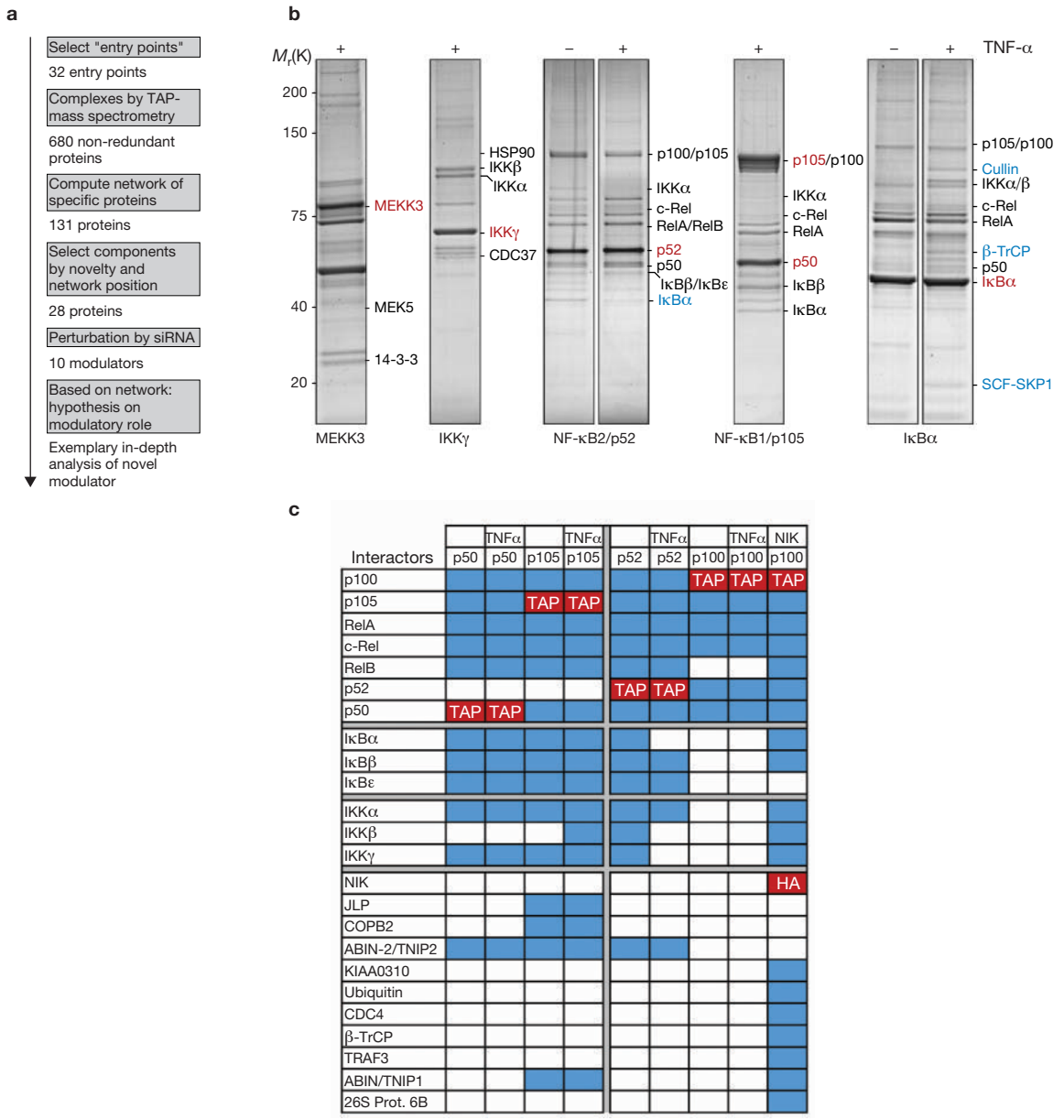


**Figure 1** Purification of cellular NF-κB/IκB complexes. (**a**) Flow chart of the integrated physical and functional pathway mapping process. (**b**) Colloidal Coomassie-stained SDS–PAGE lanes showing tandem affinity-purified MEKK3, IKKγ, NF-κB2/p52, NF-κB1/p105 and IκBα complexes from control and TNF-α-stimulated HEK293 cells. TAP-tagged proteins are indicated in red, stimulus-dependent interactors in blue and all other known interactors in black. (**c**) Stimulus-dependent interaction of proteins with the transcription factor precursors p105 and p100 and their processed forms p50 and p52. TAP-tagged entry points and HA-NIK are marked in red; all other proteins identified by LC–MS/MS in respective purifications are marked in blue.

(ref. 11). A unique feature of NF-κB activation is that the active DNA-binding-competent subunits are generated by proteasome-mediated proteolytic processing, which is regulated by sequential post-translational modifications and an ill-defined co-translational mechanism[12,13]. We observed the specific recruitment of proteins to NF-κB2/p100 in response to NIK overexpression, recapitulating the sequence of events during processing (Fig. 1c). Besides known factors such as NIK itself, IKK subunits (in particular IKKα), β-TrCP (β-transducin repeat-containing protein) and the 26S proteasomal subunit S6, we identified another F-box protein, CDC4, suggesting the involvement of an alternative SCF E3 ubiquitin ligase (Fig. 1c)[4,5,14,15]. For NF-κB1/p105, as expected, only constitutive interactors were identified, including new ones such as JLP, COPB2 and ABIN (Fig. 1c). Although most ribosomal proteins often contaminate purifications because of their cellular abundance and are filtered out, we found that three particular ribosomal proteins specifically and exclusively co-purified with NIK and/or p52. This finding raises the intriguing possibility that specific interactions with ribosomal components might account for the co-translational generation of mature NF-κB/p52 subunits[16].

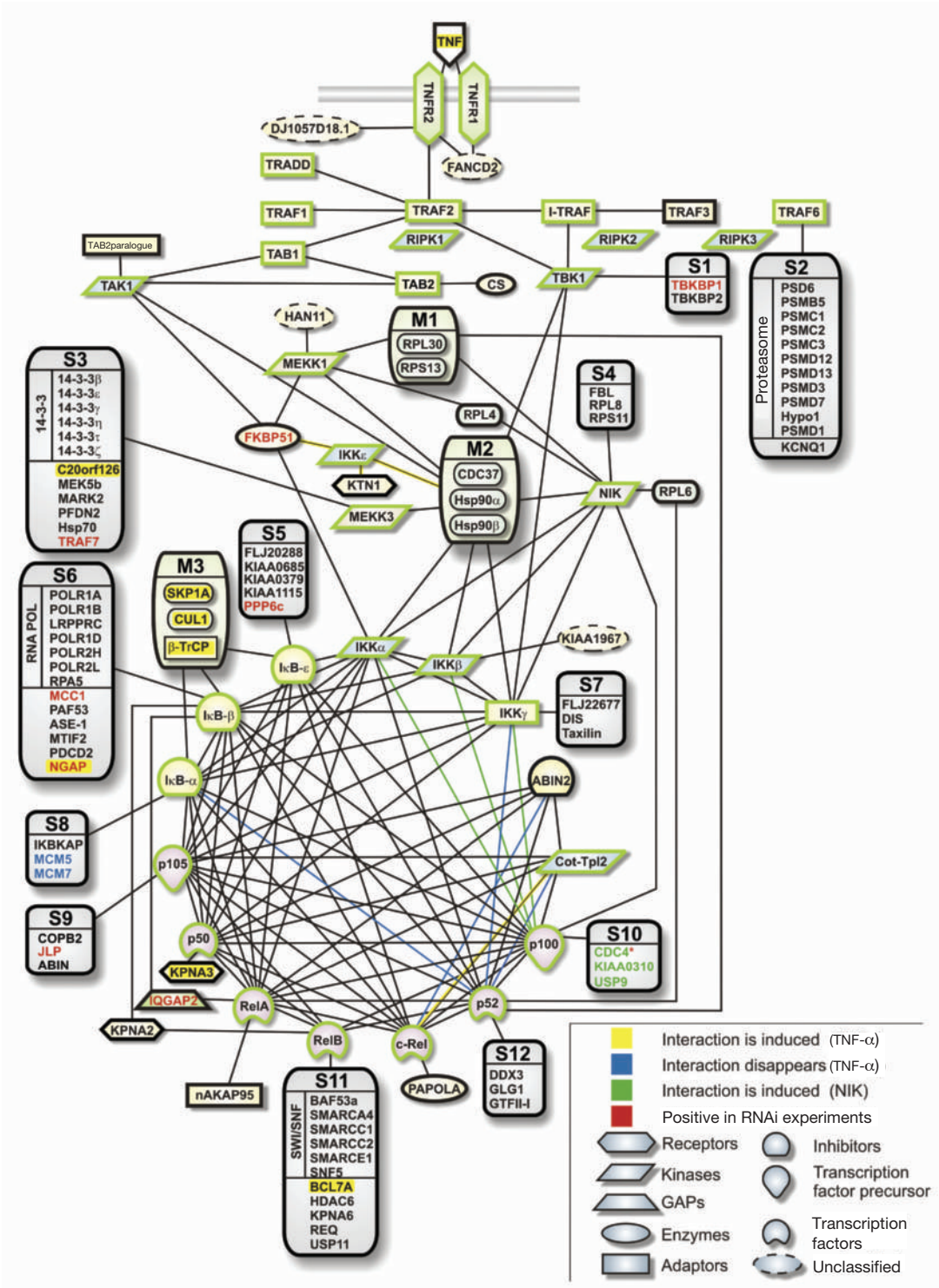


**Figure 2** Connectivity map of the TNF-α/NF-κB signal transduction pathway. The pathway is visualized as a network in which proteins are represented as shapes and colours that indicate a functional category (for complete Alliance for Cellular Signalling convention, see http://www.signalling-gateway.org) and with lines between proteins indicating that these proteins co-purified. TAP-tagged pathway components display a green frame around their respective shapes. Proteins that are found specifically with a single TAP-tagged pathway component are grouped in boxes labelled specific (S1 to S12), whereas proteins that are consistently found together with more than one TAP-tagged component and therefore represent modular components of the pathway are grouped in boxes denoted modular (M1 to M3). Proteins marked red scored positive in RNAi experiments, interactions highlighted in yellow were induced after stimulation with TNF-α, interactions indicated in blue disappeared after stimulation with TNF-α, and interactions induced by NIK are highlighted in green.

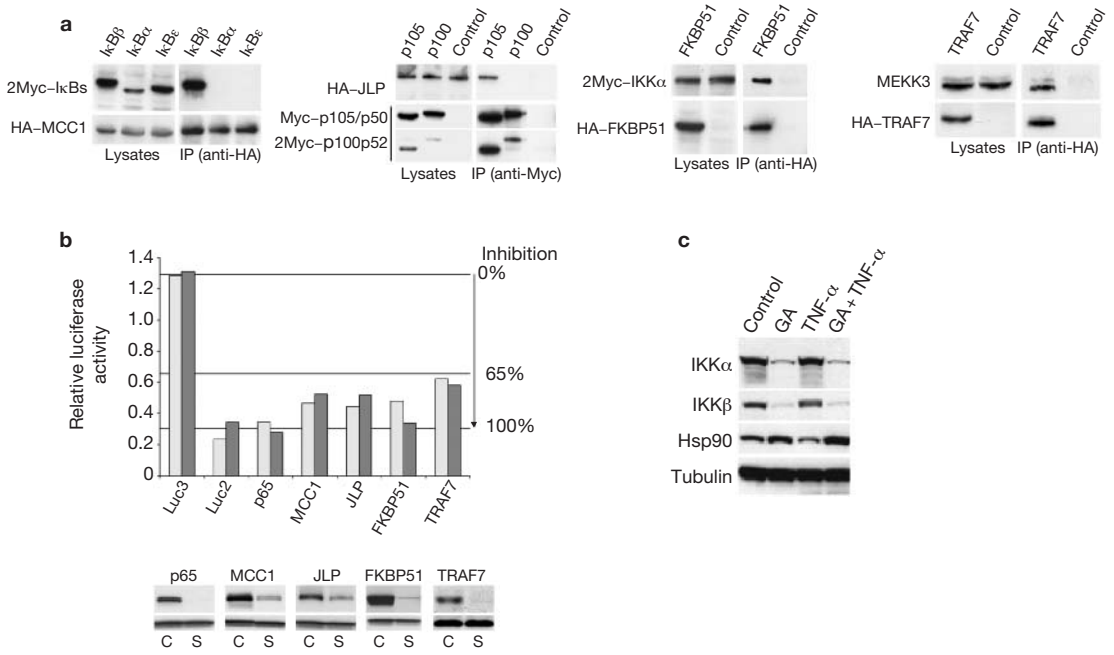


**Figure 3** Functional validation of candidate modulators of the TNF-α/NF-κB pathway. (**a**) Confirmation of interactions by co-immunoprecipitations in HEK293 cells; from left to right: HA–MCC1 and 2Myc–IκBβ; HA–JLP and Myc–p105/p50 or 2Myc–p100/p52; HA–FKBP51 and 2Myc–IKKα; HA–TRAF7 and endogenous MEKK3. IP, immunoprecipitation. (**b**) Top: RNAi of p65, MCC1, JLP, FKBP51 and TRAF7 expression reduces NF-κB activation measured in a luciferase reporter assay. Results of two independent experiments are shown; 100% inhibition corresponds to p65 RNAi. Bottom: efficacy of RNAi was checked in all cases by specific depletion of the coexpressed corresponding HA-tagged target (c, control RNAi duplex; s, specific RNAi duplex) compared with a marker protein. (**c**) Geldanamycin (GA) induces degradation of IKKα and IKKβ. HeLa cells were treated with 500 nM GA for 13 h and/or with 10 ng ml$^{-1}$ TNF-α for 12 min. Levels of endogenous proteins were detected with specific antibodies.

## A functional map

On the basis of network exploration and sequence analysis, we selected 28 components distributed over the connectivity graph for functional validation. We performed systematic single gene expression perturbations using RNAi, employing four different oligonucleotides (oligos) per gene and monitored the phenotypic effect on an NF-κB-dependent luciferase reporter read-out. In this assay, a 'loss-of-function' phenotype was scored if RNAi of at least 1 oligo per gene resulted in more than 65% inhibition (normalized to the maximal inhibition observed with RNAi against p65). RNAi with 10 of the 28 candidates showed a reproducible decrease in luciferase activity consistent with a modulatory role in TNF-α/NF-κB signal transduction (Table 1). Two of those had no previous functional annotation, FLJ33305 (which we termed TRAF7) and KIAA0775 (which we named TBKBP1, for TBK1-binding protein 1). On the basis of the position in the connectivity graph and the biochemical function of each of these 10 interactors a testable hypothesis on the respective modulatory role can be proposed.

## MCC1

MCC1 (Mutated in Colorectal Cancer) is a coiled-coil protein, proposed to be involved in cell-cycle regulation, that interacted specifically with IκBβ (Fig. 3a)[17,18]. Epitope-tagged MCC1 is localized in cytosolic structures and distributes throughout the cytoplasm after IκBβ coexpression (data not shown). On overexpression, MCC1 stabilized exogenous and endogenous IκBβ; conversely, RNAi of MCC1 destabilized endogenous IκBβ (data not shown). The former effect is similar to the overexpression of κB–Ras1 and κB–Ras2, raising the intriguing possibility that these proteins might be part of an alternative cytosolic retention mechanism for NF-κB (ref. 11).

## JLP

JLP (JNK-associated leucine zipper protein) is a kinase scaffold that might juxtapose MAP kinase modules and target transcription factor substrates[19]. JLP interacted reciprocally with NF-κB1/p105 but not NF-κB2/p100 (Fig. 3a). RNAi of JLP expression resulted in decreased NF-κB activity in response to treatment with TNF-α. This indicates that JLP might be involved in specifically directing a p105-related modification by scaffolding JNK and p38 MAP kinase and their respective upstream MAPKKs and substrates (Fig. 3b).

## FKBP51

FK506-binding protein 51 (FKBP51) is a heat shock protein (Hsp)90-binding immunophilin with peptidylprolyl isomerase activity[20]. FKBP51 co-purified with IKKα, IKKε, TAK1 and MEKK1, and the interaction with IKKα was confirmed by co-immunoprecipitation (Fig. 3a). In addition, the reciprocal purification of TAP-tagged FKBP51 resulted in the identification of endogenous IKKα and several other kinases, indicating that FKBP51 might be a prominent multifunctional kinase cofactor (data not shown). The results obtained with RNAi of FKBP51 indicate an essential role in the overall signalling process (Fig. 3b).

## Hsp90–CDC37

The Hsp90–CDC37 chaperone complex has been implicated in the maturation of kinases and the IKKα,β,γ complex[21]. Pharmacological inhibition of Hsp90–CDC37 by geldanamycin inhibits the TNF-α-mediated activation of NF-κB and, contrary to previous observations, led to degradation of the IKKα and IKKβ subunits (Fig. 3c)[21]. Under these conditions, geldanamycin treatment also destabilized the known

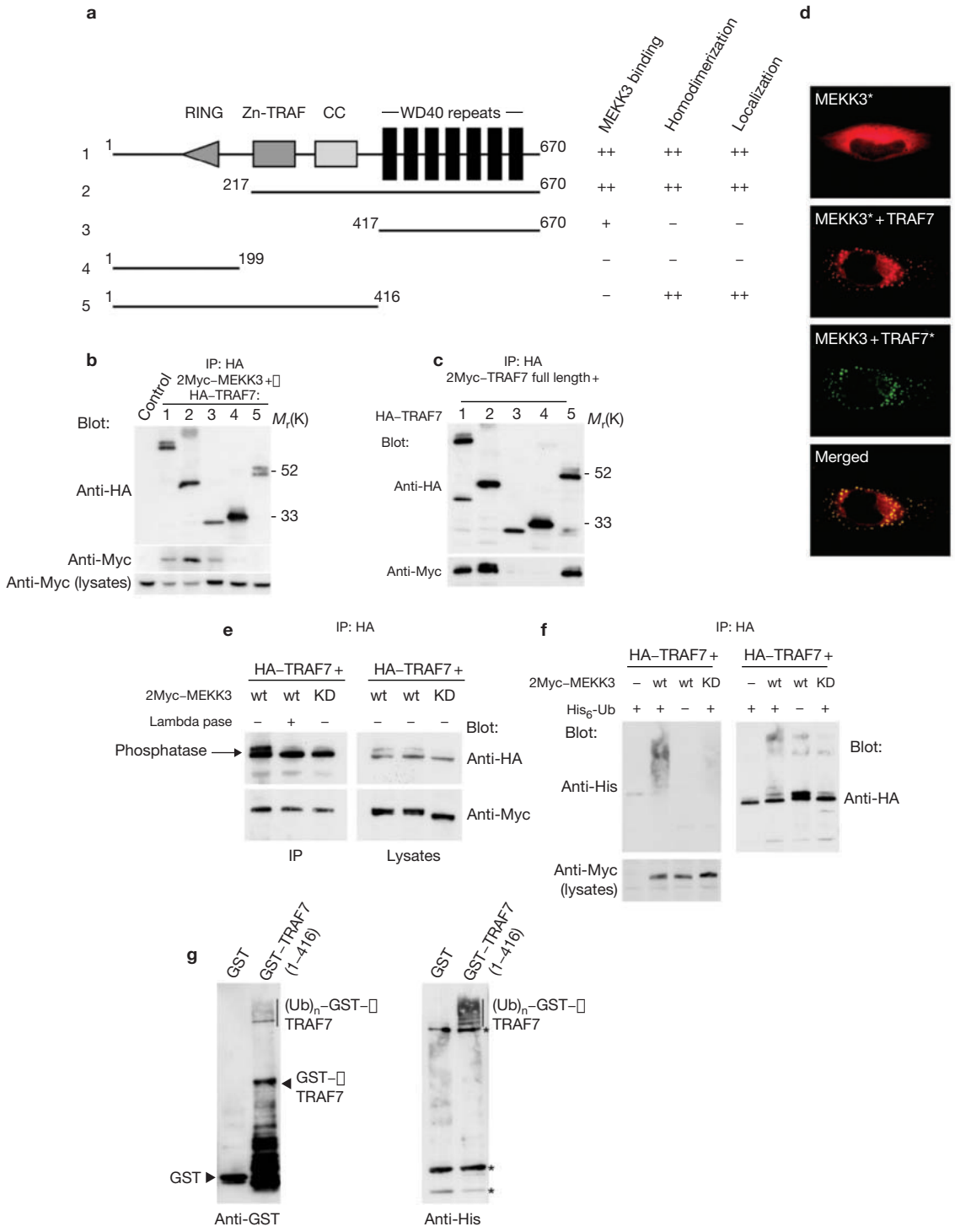


**Figure 4** TRAF7 is phosphorylated and ubiquitinated in a MEKK3-dependent manner. (**a**) Schematic representation of TRAF7 and different deletion mutants. The RING finger (RING), Zn-TRAF and coiled-coiled (CC) domains and the seven WD40 repeats are indicated. Results of MEKK3 binding to TRAF7, TRAF7 homodimerization and immunofluorescence localization studies of TRAF7 to vesicle-like structures are summarized at the right. (**b**) TRAF7 binding to MEKK3 is mediated by the WD40 repeats. IP, immunoprecipitation. (**c**) The Zn-TRAF7/CC region is required for homodimerization. (**d**) Ectopically expressed tagged MEKK3 and TRAF7 co-localized in vesicle-like structures in HeLa cells. Note the redistribution of MEKK3 when TRAF7 is coexpressed. The asterisk denotes the protein that is detected by immunofluorescence. (**e**) TRAF7 is phosphorylated by MEKK3. Immunoprecipitates of TRAF7 containing wild-type (wt) or kinase-dead (KD, K387M) MEKK3 were treated or not with phage lambda phosphatase. (**f**) TRAF7 is ubiquitinated in a MEKK3-dependent manner. HA–TRAF7, 2Myc–MEKK3 and $His_6$–polyubiquitin were all expressed in HEK293 cells. TRAF7 was immunoprecipitated and ubiquitination was detected with an anti-His antibody. (**g**) TRAF7 acts as an E3 ligase. Bacterially purified GST–TRAF7 (amino acids 1–416) or GST alone was incubated with E1 and E2 enzymes and His-ubiquitin, and ubiquitination was detected by western blotting; asterisks denote unspecific bands.

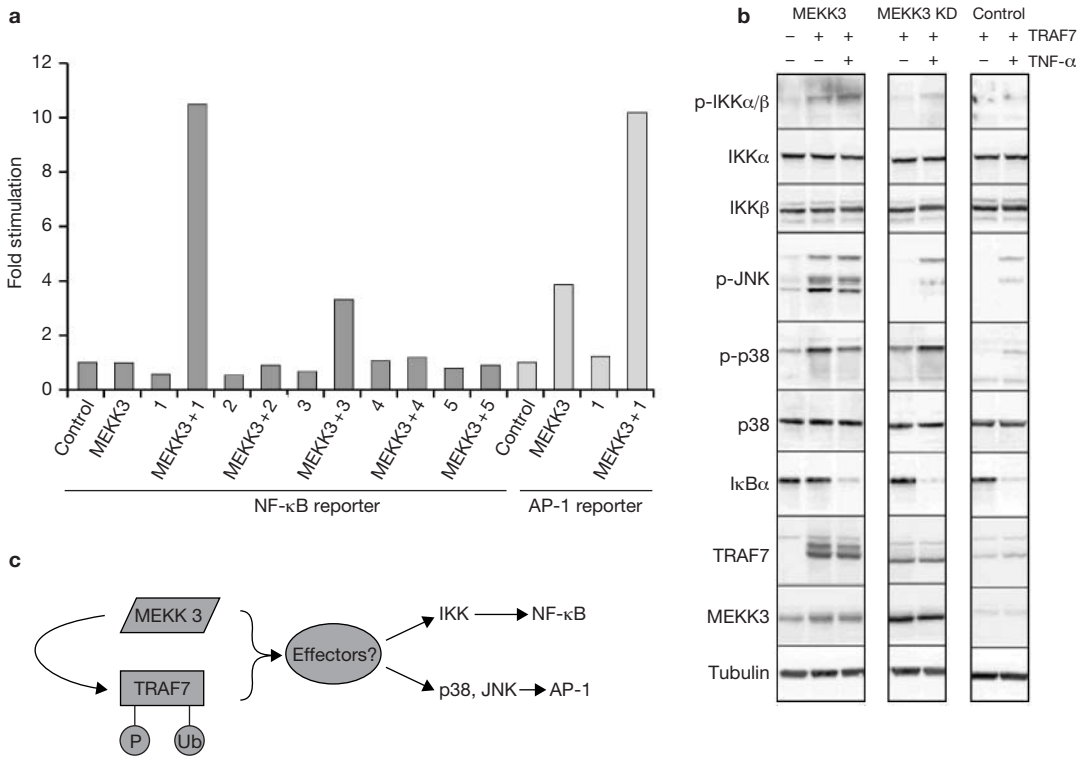


**Figure 5** MEKK3 and TRAF7 synergize to activate NF-κB, p38 and JNK pathways. (**a**) Activation of NF-κB and AP-1 luciferase reporter by single expression or coexpression of 2Myc–MEKK3, HA–TRAF7 (1) or different TRAF7 deletion mutants (2–5). (**b**) Coexpression of MEKK3 and TRAF7 results in the activation of JNK and p38 MAP kinases. HEK293 cells were transfected to express HA–TRAF7 and/or 2Myc–MEKK3. Cells were treated with TNF-α for 12 min. Protein levels and phosphorylation events were detected by specific antibodies, except for TRAF7 and MEKK3 which were detected by anti-HA and anti-Myc antibodies, respectively. (**c**) Model depicting the possible synergism of MEKK3 and TRAF7 leading to activation of the NF-κB, p38 and JNK pathways.

Hsp90-dependent kinases HER2 and RIP1, whereas other proteins, such as IκBα and NF-κB1/p105, remained unaffected. Nevertheless, we cannot exclude the possibility that the observed degradation of Hsp90 client proteins is due in part to a decrease in their respective messenger RNA concentrations, because geldanamycin has profound antiproliferative and ultimately cytotoxic effects. Our TAP analysis revealed that most kinases in the pathway associate with this dimeric chaperone, presumably during their maturation or activation process, implying that geldanamycin and its derivatives might therefore have a more pleiotropic mechanism of action than previously expected. Interestingly, we observed that IκB-associated IKKα,β,γ subunits are devoid of CDC37. In contrast, the TAP purification of all three core IKK subunits resulted in the identification of this kinase chaperone complex, suggesting distinct roles for different IKKα,β,γ subcomplexes and a 'priming' role for Hsp90–CDC37.

## TRAF7

TRAF7 is a 670-amino-acid new member of the TRAF family with a modular structure: at the N terminus it contains a RING finger domain followed by a non-canonical TRAF domain, a coiled-coil (CC) domain and seven carboxy-terminal WD40 repeats (Fig. 4a). TRAF7 was specifically identified with TAP-tagged MEKK3, a MAPKKK required for the TNF-α-induced activation of NF-κB[22]. To determine whether endogenous MEKK3 interacted with TRAF7, we performed co-immunoprecipitation experiments with epitope-tagged TRAF7. Endogenous MEKK3 was specifically co-immunoprecipitated with haemagglutinin (HA)-tagged TRAF7 from HEK293 cell lysates (Fig. 3a). To delineate the MEKK3 interaction domain we generated a series of N- and C-terminal deletion mutants (denoted 2–5) and performed co-immunoprecipitations from co-transfected HEK293 cells. The minimal TRAF7 domain sufficient for MEKK3 binding was mapped to the seven WD40 repeats (Fig. 4b). During the course of these experiments we observed homodimerization of TRAF7. The domain sufficient for homodimerization was mapped to the central region, containing the TRAF and CC domains (Fig. 4c). Next we determined the subcellular localization of ectopically expressed TRAF7 and the mutant versions. HA-tagged TRAF7 and the mutants 2 and 5 are localized in a vesicular pattern in the cytosol, indicating that this compartmentalization is dependent on the homodimerization domain. Coexpression of MEKK3 and TRAF7 resulted in a redistribution of MEKK3 to such cytosolic vesicular structures supportive of a functional interaction (Fig. 4d). We noted that coexpression resulted in a more slowly migrating TRAF7 species in SDS–polyacrylamide-gel electrophoresis (SDS–PAGE), indicative of MEKK3-dependent phosphorylation. To test this hypothesis, we coexpressed either wild-type or kinase-dead MEKK3 and treated samples with phosphatase to revert any phosphorylation event. Both versions of MEKK3 interacted with TRAF7, but only wild-type MEKK3 induced a more slowly migrating species that could be reverted by phosphatase treatment, indicating that TRAF7 is phosphorylated by MEKK3 (Fig. 4e). Both wild-type TRAF7 and mutant 5 seem to be modified post-translationally by MEKK3, indicating that the major phoshorylation sites might be located in the N-terminal region. As well

as phosphorylation, we observed high-molecular-mass TRAF7 species, indicating possible additional modifications such as ubiquitination. To investigate this possibility we coexpressed MEKK3 and TRAF7 together with His-tagged ubiquitin and performed co-immunoprecipitation experiments. Only wild-type MEKK3, and not the kinase-dead mutant, induced ubiquitination of TRAF7, indicating that phosphorylation might trigger ubiquitination. Interestingly, this did not result in the proteolytic degradation of TRAF7 but seemed to stabilize TRAF7 (Fig. 4f, and data not shown). Because TRAF7 contains an E3 RING finger, we next tested for auto-ubiquitination *in vitro*. In the presence of E1 and E2 activating and conjugating enzymes, a glutathione *S*-transferase (GST)-purified fragment of TRAF7, which harbours the RING domain, is ubiquitinated, indicating that TRAF7 might have E3 ubiquitin ligase activity (Fig. 4g).

To determine further the functional role of TRAF7 in the NF-κB pathway, we performed gain-of-function experiments. Overexpression of TRAF7 or any of the deletion mutants alone did not activate an NF-κB-driven luciferase reporter. However, coexpression of wild-type TRAF7, but not any of the mutants, with MEKK3 resulted in the synergistic activation of both NF-κB (20-fold) and activator protein 1 (AP-1) (3-fold) reporter constructs (Fig. 5a). In both cases synergistic activation was dependent on the kinase activity of MEKK3 (data not shown). Conversely, RNAi-mediated knockdown of TRAF7 expression inhibited the activation of NF-κB in response to stimulation with TNF-α (Fig. 3c). To delineate the signal transduction mechanism we checked for the activation of endogenous IKKα/β and the MAP kinases p38 and JNK with the use of phospho-specific antibodies. Coexpression resulted in a robust activation of JNK, which is dependent on the kinase activity of MEKK3. In contrast, p38 MAP kinase was strongly activated by coexpression of TRAF7 with wild-type MEKK3, but also weakly by coexpression with the kinase-dead mutant (Fig. 5b). The IKK subunits are only marginally activated without resulting in a detectable degradation of IκBα (Fig. 5b, rows 2, 3 and 7).

To identify potential substrates of TRAF7 we employed the TAP strategy. Purification of TRAF7 in this manner led, in addition to the identification of MEKK3, to the identification of several potential effectors with a link to ubiquitination and proteins involved in the control of epithelial cell growth and polarity, such as Scribble and Discs large (data not shown). Intriguingly, the latter two proteins are targeted for ubiquitination by the E6 oncoprotein of human papilloma virus[23].

Collectively, these data indicate an important role for TRAF7 in regulating the signalling properties of MEKK3 and in the activation of NF-κB and AP-1. Given its similarity to E3 ubiquitin ligases, we propose that TRAF7, in conjunction with MEKK3, might act like TAK1 and TRAF6 in relaying signals, impinging on the activation of JNK and p38 MAP kinase, presumably by means of intermediate effectors (Fig. 5c)[24].

## DISCUSSION

Combining large-scale pathway mapping with loss-of-function analysis as an integrated approach has allowed the identification of several newly observed modulatory components of the TNF-α/NF-κB signal transduction pathway. A physical map of the proteins in a pathway instructed a focused validation strategy and permitted the mechanistic interpretation of the resulting data. The approach is applicable to the study of any therapeutically relevant signal transduction process. Single perturbation with small-interfering RNA (siRNA) mimics pharmacological treatment in some respects and can therefore be used to model the effects of inhibiting drug targets and to choose the most effective and specific intervention strategy. We are currently employing double perturbations with RNAi to elucidate the epistatic order and to reveal potential redundant mechanisms in the signalling cascade.

## METHODS

**Tandem affinity purification and mass spectrometry.** Retroviral transduction vectors were generated by cloning open reading frames, amplified by polymerase chain reaction, into a Moloney-based vector with the Gateway site-specific recombination system (Life Technologies). N-terminal fusions were generated as a rule, except for TNFR1, TNFR2, TRADD, TRAF1, TRAF2, TRAF6, RIPK1, RIPK2, RIPK3, MEKK1, MEKK3, NIK, NF-κB2/p52 and IκBα, for which both N- and C-terminal fusions were generated. Virus stocks were generated in a HEK293 Gag–Pol packaging cell line. HEK293 cells were infected and complexes were purified by using a modified TAP protocol[1], except for MEKK1 and Cot/Tpl-2, which were transiently transfected. The proper localization of all TAP-tagged proteins was monitored by indirect immunofluorescence. Cells were grown in DMEM medium with 10% FCS. For stimulation the medium was replaced with either fresh medium containing 10 ng $ml^{-1}$ TNF-α or fresh medium alone. For Nik stimulation, HEK293 cells expressing NFκB/p100 were transiently transfected with an HA-tagged Nik construct. For the receptor-proximal components (TNFR1, TNFR2, TRAF1, TRAF2, TRAF6, iTRAF and TRADD) and the kinases (RIPK1, RIPK2, RIPK3, MEKK1, MEKK3, NIK, Cot-Tpl2, TAK1, TAB1, TAB2, TBK1, IKKα, IKKβ and IKKγ) we conducted stimulation for 10 min (except for IKKε, for which we conducted stimulation for 12 h). For downstream transduction components, we performed stimulation as follows: NF-κB1 (p105/p50), NF-κB2 (p100/p52), RelA, RelB, c-Rel, 30 min; IκBα, 10 and 30 min; IκBβ and IκBε, 10 and 60 min. Cells were harvested by mechanical detachment, washed with excess PBS on ice and lysed in immunoprecipitation buffer. Protein samples were separated by SDS–PAGE, complete gel lanes were systematically cut into slices and proteins were digested in-gel with trypsin as described[25]. Protein identification was performed by LC–MS/MS, and MS data were searched against an in-house curated version of the International Protein Index (IPI), maintained at the EBI (Hinxton, UK). Results of database searches were read into a database system for further bioinformatics analysis.

**Data analysis.** The raw data set of interactions was filtered against a control data set of purifications performed in the same cell type with proteins unrelated to the TNF-α/NF-κB pathway. Frequencies of specific interactors were tested against the null hypothesis of the background frequency of the control data set with a binomial test (*P* cut-off at $10^{-7}$). We also included interactors that seemed to come consistently with some entry points of the control data set by using an exact Fisher's test on the contingency table on the basis of all purifications (*P* cut-off at $10^{-3}$). Threshold *P* values were chosen to stay below a discontinuity jump in the ratio of accepted interactions to recovered known interactions. Homology-based searches were performed with the BLAST and PSI-BLAST algorithms. Structural attributes for each component were assessed with SMART and Pfam for conserved functional domains.

**Co-immunoprecipitations, immunofluorescence, antibodies and reagents.** Co-immunoprecipitations were performed from lysates of transiently transfected HEK293 cells expressing HA- or 2Myc-tag proteins. Indirect immunofluorescence was performed on HeLa cells transiently transfected with epitope-tagged proteins. The primary antibodies used were anti-IKKα, -IKKβ or -IKKγ (Upstate), anti-Hsp90 (BD), anti-MEKK3 (BD), anti-IκBα (Santa Cruz), anti-IκBβ (Abcam and Santa Cruz), anti-JNK, anti-(phospho p38), anti-(phospho JNK), anti-(phospho IKKα/β) (all four from Cell Signalling), anti-α-tubulin (Sigma), anti-HA (Roche); anti-Myc (Roche), anti-His (Pharmacia) and anti-GST (Santa Cruz); anti-p38 antibody was a gift from A. Nebreda (EMBL, Heidelberg). The secondary antibodies used were: anti-rabbit and anti-mouse IgG (Jackson Laboratories). His-ubiquitin, phage lambda phosphatase, TNF-α and geldanamycin were purchased from Sigma. The E1 and E2 enzymes were from BostonBiochem.

**Reporter assays and RNAi.** For loss-of-function assays, HEK293 cells were plated at a confluency of $3 \times 10^4$ cells per well of a 96-well plate 6–10 h before transfection. For every gene, four distinct siRNA duplexes (Dharmacon) were co-transfected at 10 or 20 nM with 66 ng pNF-κB–luciferase (Stratagene) reporter plasmid, 3.2 ng ubiquitin promoter–*Renilla* luciferase expression plasmid as internal standard, and 66 ng pBluescript (Stratagene) per well using Lipofectamine 2000 (Invitrogen), in accordance with the manufacturer's

instructions. At 40 h after the start of transfection, cells were either stimulated with TNF-α at 10 ng ml$^{-1}$ or mock-treated for 6 h before cell lysis at 46 h and subsequent measurement of NF-κB activity with the Dual-Glo Luciferase Assay System (Promega). In contrast, for measuring siRNA effectiveness, HEK293 cells were plated at $10^6$ cells per well into six-well plates before co-transfection of siRNA duplexes at 20 nM with 0.5 μg of a construct expressing the HA-tagged protein and 2.8 μg plasmid expressing a marker protein. At 34 h after the start of transfection, cells were harvested, and Western blot analysis was performed. For gain-of-function studies, Jurkat cells were co-transfected with tagged MEKK3 and TRAF7 expression constructs, together with a pNF-κB–luciferase or a AP-1 luciferase reporter plasmid.

*Note: Supplementary Information is available on the Nature Cell Biology website.*

ACKNOWLEDGEMENTS

We thank all our colleagues at Cellzome, in particular, G. Stark and M. Boesche with their teams, and C. Gaessler, P. Voelkel, E. M. Lorenz and H. Wilkinson for technical expertise. We thank A. Rowley and D. Brown for continuous support, M. Pasparakis and A. Nebreda for input throughout this project, and F. Weisbrodt for graphical support.

COMPETING FINANCIAL INTERESTS

The authors declare that they have no competing financial interests.

Received 23 September 2003; accepted 22 December 2003;

1. Gavin, A. C. *et al.* Functional organization of the yeast proteome by systematic analysis of protein complexes. *Nature* **415,** 141–147 (2002).
2. Ghosh, S. & Karin, M. Missing pieces in the NF-κB puzzle. *Cell* **109** (Suppl.), S81–S96 (2002).
3. Ghosh, S., May, M. J. & Kopp, E. B. NF-κB and Rel proteins: evolutionarily conserved mediators of immune responses. *Annu. Rev. Immunol.* **16,** 225–260 (1998).
4. Xiao, G., Harhaj, E. W. & Sun, S. C. NF-κB-inducing kinase regulates the processing of NF-κB2 p100. *Mol. Cell* **7,** 401–409 (2001).
5. Senftleben, U. *et al.* Activation by IKKα of a second, evolutionary conserved, NF-κB signaling pathway. *Science* **293,** 1495–1499 (2001).
6. Rigaut, G. *et al.* A generic protein purification method for protein complex characterization and proteome exploration. *Nature Biotechnol.* **17,** 1030–1032 (1999).
7. Chen, C. Y. *et al.* AU binding proteins recruit the exosome to degrade ARE-containing mRNAs. *Cell* **107,** 451–464 (2001).
8. Kemmeren, P. *et al.* Protein interaction verification and functional annotation by integrated analysis of genome-scale data. *Mol. Cell* **9,** 1133–1143 (2002).
9. von Mering, C. *et al.* Comparative assessment of large-scale data sets of protein–protein interactions. *Nature* **417,** 399–403 (2002).
10. Saccani, S., Pantano, S. & Natoli, G. Modulation of NF-κB activity by exchange of dimers. *Mol. Cell* **11,** 1563–1574 (2003).
11. Fenwick, C. *et al.* A subclass of Ras proteins that regulate the degradation of IκB. *Science* **287,** 869–873 (2000).
12. Dixit, V. & Mak, T. W. NF-κB signaling. Many roads lead to Madrid. *Cell* **111,** 615–619 (2002).
13. Mordmuller, B., Krappmann, D., Esen, M., Wegener, E. & Scheidereit, C. Lymphotoxin and lipopolysaccharide induce NF-κB–p52 generation by a co-translational mechanism. *EMBO Rep.* **4,** 82–87 (2003).
14. Fong, A., Zhang, M., Neely, J. & Sun, S. C. S9, a 19 S proteasome subunit interacting with ubiquitinated NF-κB2/p100. *J. Biol. Chem.* **277,** 40697–40702 (2002).
15. Fong, A. & Sun, S. C. Genetic evidence for the essential role of beta-transducin repeat-containing protein in the inducible processing of NF-κB2/p100. *J. Biol. Chem.* **277,** 22111–22114 (2002).
16. Heusch, M., Lin, L., Geleziunas, R. & Greene, W. C. The generation of NFκB2 p52: mechanism and efficiency. *Oncogene* **18,** 6201–6208 (1999).
17. Kinzler, K. W. *et al.* Identification of a gene located at chromosome 5q21 that is mutated in colorectal cancers. *Science* **251,** 1366–1370 (1991).
18. Matsumine, A. *et al.* MCC, a cytoplasmic protein that blocks cell cycle progression from the G0/G1 to S phase. *J. Biol. Chem.* **271,** 10341–10346 (1996).
19. Lee, C. M., Onesime, D., Reddy, C. D., Dhanasekaran, N. & Reddy, E. P. JLP: A scaffolding protein that tethers JNK/p38MAPK signaling modules and transcription factors. *Proc. Natl Acad. Sci. USA* **99,** 14189–14194 (2002).
20. Nair, S. C. *et al.* Molecular cloning of human FKBP51 and comparisons of immunophilin interactions with Hsp90 and progesterone receptor. *Mol. Cell. Biol.* **17,** 594–603 (1997).
21. Chen, G., Cao, P. & Goeddel, D. V. TNF-induced recruitment and activation of the IKK complex require Cdc37 and Hsp90. *Mol. Cell* **9,** 401–410 (2002).
22. Yang, J. *et al.* The essential role of MEKK3 in TNF-induced NF-κB activation. *Nature Immunol.* **2,** 620–624 (2001).
23. Humbert, P., Russell, S. & Richardson, H. Dlg, Scribble and Lgl in cell polarity, cell proliferation and cancer. *BioEssays* **25,** 542–553 (2003).
24. Wang, C. *et al.* TAK1 is a ubiquitin-dependent kinase of MKK and IKK. *Nature* **412,** 346–351 (2001).
25. Shevchenko, A., Wilm, M., Vorm, O. & Mann, M. Mass spectrometric sequencing of proteins silver-stained polyacrylamide gels. *Anal. Chem.* **68,** 850–858 (1996).

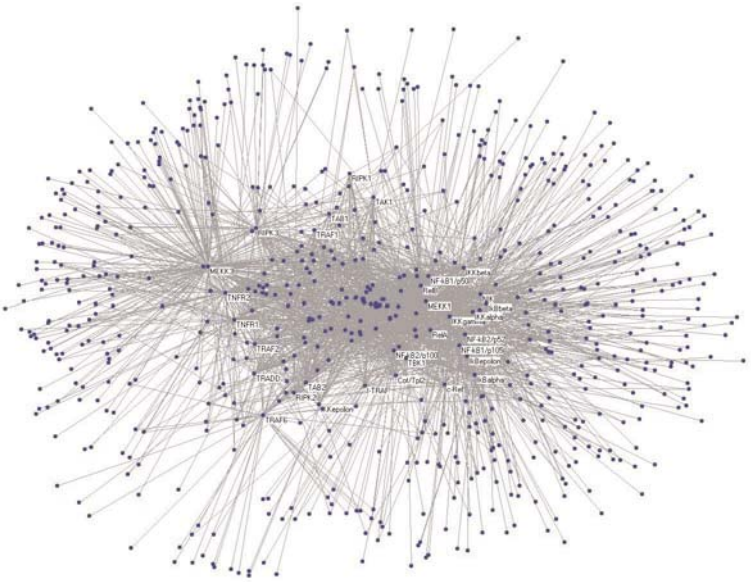

Figure S1. Connectivity graph of all 680 non-redundant proteins